Progress In Electromagnetics Research, Vol. 140, 491–508, 2013

NON-LINEAR OPTIMIZATION OF AN INJECTION LOCKED HIGH EFFICIENCY VCO WITH ARBITRARILY WIDTH MODULATED MICROSTRIP LINE NETWORKS

Marta Gonzalez*, Samuel Ver Hoeye, Miguel Fernandez, Carlos Vazquez, George R. Hotopan, Rene Camblor, and Fernando Las Heras

Department of Electrical Engineering, University of Oviedo, Campus Universitario de Viesques, Gijon E-33203, Spain

Abstract—In this work a non-linear efficiency optimization method for its application to an Injection-Locked High Efficiency Voltage Controlled Oscillator is presented. The proposed approach is based on the control of the harmonic content of the oscillator autonomous signal, which is accomplished through the use of an Auxiliary Generator and several multi-harmonic loads based on Arbitrarily Width-Modulated Microstrip Lines. The presented technique has been applied to the design of a 2.5 GHz high efficiency Voltage Controlled Oscillator, which has been manufactured and experimentally characterized, obtaining a good agreement between the simulated and measured results.

1. INTRODUCTION

In addition to purely technical specifications, modern systems have to accomplish with hard requirements about size, weight, cost and power consumption, specially when considering battery powered mobile applications. Oscillators play a key role in such communication systems as they condition their characteristics and, together with power amplifiers, are one of the main power demanding system blocks.

Power efficiency is a critical specification from the point of view of components, devices and systems [1–3]. The use of high efficiency devices involves lower DC power consumption, increases the lifetime of the batteries, simplifies the management of thermal issues [4] and reduces their cost. In addition, when working with solid state

Received 26 April 2013, Accepted 31 May 2013, Scheduled 18 June 2013

* Corresponding author: Marta Gonzalez Corredoiras (martagcorredoiras@gmail.com).

microwave transistors, low DC operation voltages are preferred, since the necessary DC power is reduced.

Several works addressing the optimization of the efficiency in microwave amplifiers have been reported in technical literature [5–8]. However, the described techniques cannot be directly applied to the design of oscillators, due to fact that the power, the frequency and the stability of the autonomous signal have to be simultaneously controlled. Specific efficiency optimization techniques for microwave oscillators have also been developed [9–18]. Some of them are applied to optimize fixed frequency oscillators. In other cases, the proposed techniques address the optimization of high DC bias voltage transistor based devices. Furthermore, some authors have reported the great influence of the harmonic content of the autonomous signal on the oscillator efficiency [10, 15, 19]. Therefore, the efficiency maximization can be approached in terms of the harmonic control of the circuit.

In this work, a novel non linear optimization technique for the optimization of the efficiency of a 2.5 GHz Voltage Controlled Oscillator (VCO) with low DC bias voltage is presented. It is based on the harmonic control of the autonomous signal through the inclusion of multi-harmonic loads based on Arbitrarily Width Modulated Microstrip Lines (AWMML) [20, 21]. With the proposed approach, the efficiency can be optimized while the output frequency and power are imposed by using an Auxiliary Generator (AG) [21–26]. In addition, the high design flexibility provided by AWMML based structures allows the accurate control of the circuit and avoids most of the problems related with the use of structures based on conventional transmission lines and open or short ended stubs.

Once the high efficiency VCO is designed, it will be synchronized with an external signal in order to obtain two different operation modes. On the one hand, if the frequency of the input reference signal is varied, the circuit can be used as synchronized oscillator with low phase noise. On the other hand, if a fixed frequency input signal is used, the circuit will work as electronically tunable continuous range phase shifter. In both cases, the efficiency of the synchronized solutions will be analyzed through the use of the AG technique.

2. TOPOLOGY AND NON LINEAR DESIGN OF THE VCO

2.1. Topology

The topology of the VCO is represented in Fig. 1. The circuit is based on a single ultra-low noise PHEM transistor. The feedback network at the source port provides negative resistance at the gate

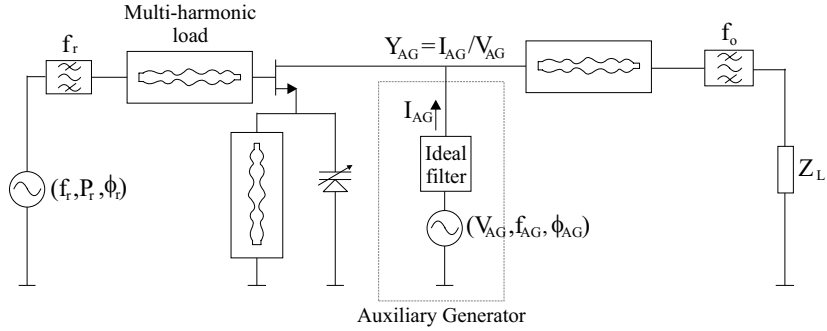

Figure 1. Topology of the VCO. The connection of the multi-harmonic loads and the Auxiliary Generator is indicated.

port and enables the existence of a self-oscillation signal with frequency $f_o = 2.5\,\text{GHz}$. This network includes a varactor diode. In the free running oscillator, the varactor allows slightly frequency tuning. Under synchronized operation, it enables the electronic control of the introduced phase shift. The input reference signal, with frequency $f_r = f_o$ and power P_r, is provided to the circuit through a band-pass filter. The output signal is obtained at the drain port of the transistor by using other band-pass filter.

Three AWMML based multi-harmonic loads are placed at the three terminals of the transistor. This kind of structure allows the precise control of its input impedance over a wide frequency range. Therefore, they are used to control in a precise way the harmonic content of the oscillator autonomous signal and to maximize its efficiency. Due to its good performance, it is also be used to design the DC bias networks.

2.2. Non Linear Design of the VCO

The large signal oscillator design process is completely based on Harmonic Balance simulations and the use of an Auxiliary Generator. At the first design stage, the autonomous signal start-up conditions [27–29] are fulfilled. Then, an Auxiliary Generator, which is placed at the drain port of the transistor and works with frequency $f_{AG} = f_o$, amplitude $V_{AG} = V_o$ and phase ϕ_{AG}, is used to impose the large signal steady-state autonomous solution. This is achieved in an optimization process in which several design parameters are modified in order to satisfy the non perturbation condition of the Auxiliary Generator [21–26]. The goals of such optimization procedure can be

mathematically expressed as:

$$\begin{cases} \Re\{Y_{AG}(f_{AG} = f_o,\ V_{AG} = V_o,\ \bar{\gamma}_c)\} = 0 \\ \Im\{Y_{AG}(f_{AG} = f_o,\ V_{AG} = V_o,\ \bar{\gamma}_c)\} = 0 \end{cases} \quad (1)$$

where Y_{AG} is the admittance seen by the Auxiliary Generator and $\bar{\gamma}_c$ the set of optimization variables.

Once the conditions indicated in (1) are fulfilled, it can be ensured that the circuit is able to maintain itself the autonomous solution defined by f_{AG}, V_{AG} and ϕ_{AG}. In addition, due to the intrinsic non linear character of the design technique, the harmonic content of the autonomous signal can be calculated and/or controlled. The efficiency ϵ, is calculated as $\epsilon = \frac{P_o}{P_{DC}}$, where P_o is the power of the autonomous signal fundamental component, evaluated at the circuit output port, and P_{DC} is the DC power consumption. At this design stage, its value is $\epsilon = 7.8\%$. The voltage and current waveforms, which have been calculated taking into account the first ten harmonic components, evaluated at the drain port of the transistor, are shown in dashed line in Fig. 4.

3. ARBITRARILY WIDTH MODULATED MICROSTRIP LINE (AWMML) NETWORKS

The structure of the AWMML based networks is schematized in Fig. 2. It is composed by the series connection of a large number N of short microstrip tapered line sections, with equal length $\Delta L = \frac{L}{N}$, where L represents the total length of the structure. Therefore, the set of parameters which defines the AWWML is formed by N, ΔL and the width pairs W_i, W_{i+1} which represent the initial and end width of the i^{th} tapered element. Note that, in order to obtain a continuous width modulation function, the end width of each element has to match with the initial width of the next one.

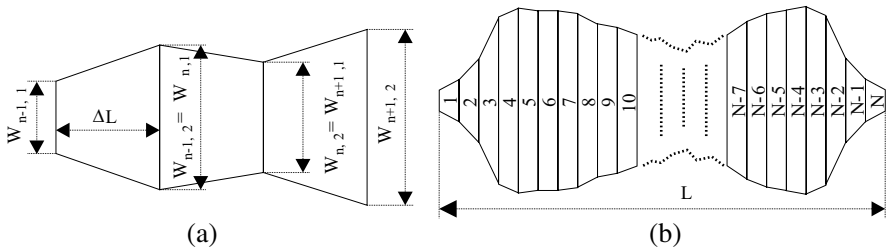

Figure 2. Bias network and multiharmonic load based on an AWMML.

The use of AWMML based structures provides some fundamental advantages whit respect to the traditional narrow band loads based on conventional transmission lines and stubs. First, the input impedance of AWMMLs can be simultaneous and accurately controlled over a wide bandwidth around several frequency points, which considerably increases the design flexibility. In addition, practical problems derived from the use of stubs, such as circuital models inaccuracy, radiation at the ends or electromagnetic coupling, are avoided. Therefore, the deviation between simulation and experimental results is reduced.

The good properties of AWMMLs make them suitable for the design of the DC bias networks. Since the oscillator efficiency is closely related to the harmonic content of the autonomous signal, the DC bias networks have to be designed to present high input impedance at the fundamental and the first harmonic components of such signal. In this way, the DC bias networks do not influence the autonomous signal harmonic content.

DC bias networks have been designed through an optimization process which involves the structure defining parameters. The goal of this process is to obtain high input impedance over a 200 MHz bandwidth centered at 2.5, 5 and 7 GHz, which corresponds to the first three harmonic components of the autonomous solution. Since the amplitude of the autonomous signal harmonic components considerably decreases as the order increases, the behavior of the DC bias network at frequencies above 7.5 GHz can be neglected without affecting the overall circuit performance. Fig. 3(a) shows the shape

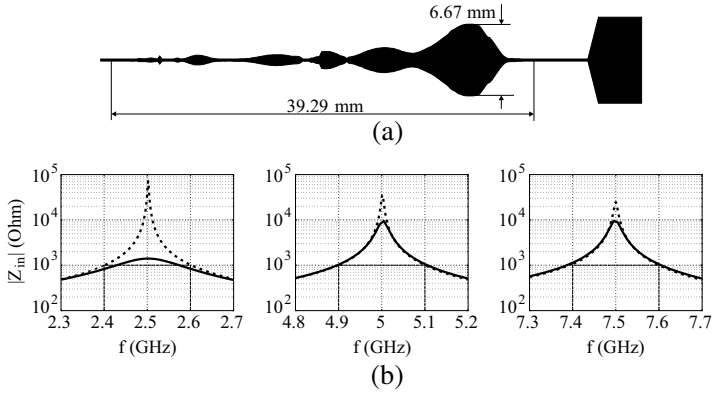

Figure 3. (a) Layout of the DC bias network. (b) Input impedance of the DC bias network, calculated through circuital (dashed line) and electromagnetic (continuous line) simulations.

of the optimized DC bias network, including an additional microstrip section to place decoupling capacitors and the bias wire. The simulated frequency response of the structure is represented in Fig. 3(b). As can be observed, a minimum $|Z_{in}|$ value of $1\,\mathrm{k}\Omega$ is obtained around the frequencies of interest. The frequency response of the structure has also been calculated using an electromagnetic simulator based on the Method of Moments. Note that the results obtained from this analysis are fully compliant with the design goals.

In the next section, the same optimization procedure will be applied to the three AWMML based multi-harmonic loads in order to maximize the efficiency of the free running VCO.

4. OPTIMIZATION OF THE FREE RUNNING VCO EFFICIENCY

Previous works [10, 15, 19] have demonstrated that the oscillator efficiency is directly related to the harmonic content of the autonomous signal and to the load seen by the transistor, since they determine the voltage and current waveforms. In these works, the efficiency optimization is performed in two steps. First, the optimum harmonic content of the autonomous signal has to be calculated. After that, it is imposed through the design of the transistor load.

In this work, a different optimization approach, which allows the direct imposition of the efficiency and does not require previous knowledge about the autonomous signal harmonic content, has been developed. The oscillator efficiency ϵ is considered as a goal of a nonlinear optimization process based on the use of an Auxiliary Generator. The set of optimization goals described in (1) is completed with the efficiency related goal as follows:

$$\begin{cases} \Re\{Y_{AG}(f_{AG} = f_o,\ V_{AG} = V_o,\ \bar{\gamma}_c)\} = 0 \\ \Im\{Y_{AG}(f_{AG} = f_o,\ V_{AG} = V_o,\ \bar{\gamma}_c)\} = 0 \\ \epsilon(f_{AG} = f_o,\ V_{AG} = V_o,\ \bar{\gamma}_c) > \epsilon_{\min} \end{cases} \tag{2}$$

where $\bar{\gamma}_c$ is composed by the variables which define the geometry of three AWMML based multi-harmonic loads, and $\epsilon_{\min}$ is the efficiency value to be reached. As the desired solution is calculated through the Harmonic Balance technique, the frequency response of the AWMML structures is implicitly evaluated at the frequencies of all the harmonic components which are used to define the Harmonic Balance frequency basis. On the other hand, the high flexibility provided by such structures ensures the convergence of the optimization process towards the desired steady-state high efficiency autonomous solution.

The simultaneous fulfillment of the conditions given in (2) ensures the existence of an autonomous signal with frequency f_o, amplitude V_o and efficiency greater than $\epsilon_{\min}$. The maximum efficiency reached with the proposed approach is $epsilon_{\max} = 44.96\%$, while the output power is $P_o = 11.3\,\text{dBm}$. The voltage and current waveforms, evaluated after the optimization process at the transistor drain port, are shown in continuous line in Fig. 4. Note that the current waveform presents a quasi square shape, and its maximum is located around the voltage

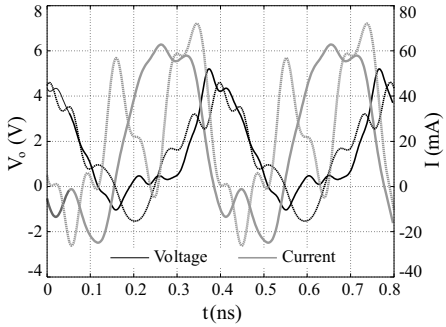

Figure 4. Voltage and current waveforms evaluated at the transistor drain port. Dashed line: before optimization. Continuous line: after optimization.

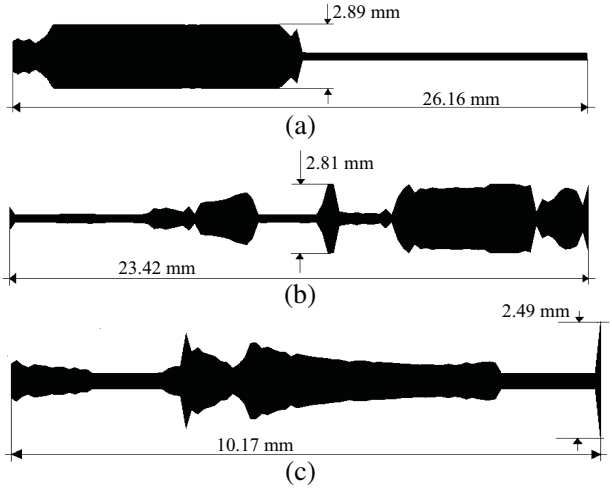

Figure 5. Layout of the AWMML based multi-harmonic load after the optimization process. (a) Gate load. (b) Source load (feedback network). (c) Drain load.

minimum, which is coherent with the previously reported results. After the optimization process, $\bar{\gamma}_c$ has been evaluated in order to generate the multi-harmonic load layouts, which have been represented in Fig. 5.

Since the efficiency value is directly imposed, the optimum harmonic content of the autonomous signal has not to be previously computed. In addition, the use of the AWMML based multi-harmonic loads ensures the optimization process convergence. Therefore, the described approach simplifies the oscillator design and optimization, while considerably reduces the required time.

5. SYNCHRONIZED SOLUTIONS OF THE HIGH EFFICIENCY VCO

One of the main drawbacks of microstrip VCOs is their inherent phase noise level, which is mainly due to the low quality factor of the circuit. This disadvantage can be overcome by synchronizing the autonomous signal with a high quality external reference signal [21]. In this section, the influence of the parameters of the reference signal on the efficiency of the synchronized solutions will be analyzed. On the other hand, the behavior of the Injection-Locked VCO (ILVCO) as electronically tunable phase shifter will be studied.

5.1. Injection Locked Behavior of the High Efficiency VCO

When the oscillator works under fundamental synchronization regime, the frequency of the autonomous signal f_o equals to that of the reference signal f_r and the phase difference between them, $\Delta\phi = \phi_o - \phi_r$, is constant in time. Since the phase of the reference signal can be arbitrarily set to zero, the phase difference between the autonomous and the reference signals can be expressed as $\Delta\phi = \phi_o = \phi_{AG}$. Therefore, the synchronized solutions are found by sweeping the phase of the Auxiliary Generator ϕ_{AG} between 0 and 360°, and calculating for each swept point the values of the amplitude $V_o = V_{AG}$ and the frequency $f_o = f_{AG} = f_r$ of the autonomous signal for which the non perturbation condition of the Auxiliary Generator is satisfied [21–26].

The synchronized solutions of the ILVCO, expressed in terms of the output power P_o, are represented in Fig. 6(a) for different values of the reference signal power P_r. For the sake of representation clarity, the different synchronization loci have been normalized with respect to their center frequency f_c. Note that only the solutions contained on the lower half of the synchronization loci are stable.

The efficiency associated to the synchronized solutions has been represented in Fig. 6(b). As can be observed, the variation of the

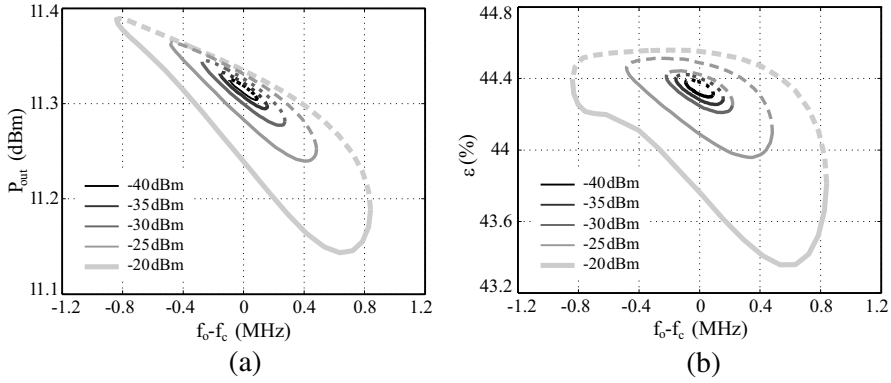

Figure 6. (a) Synchronized solutions in terms of the output power P_o, for different values of P_r. (b) Efficiency on the synchronized solutions. Continuous line: stable solutions. Dashed line: unstable solutions.

efficiency along the locking range, taking into account only the stable solutions, is less than 0.2%. On the other hand, the variation of the efficiency, evaluated at the center of the locking range, is less than 0.3% when the reference signal changes between -40 and -20 dBm. It has to be taken into account that the maximum additional power provided to the oscillator by the reference source, i.e., $P_r = -20$ dBm, is negligible when compared with the power of the output signal.

Figure 7 represents the voltage waveform, evaluated at the transistor drain port, corresponding with three different synchronized solutions, obtained with $P_r = -25$ dBm. The selected working points

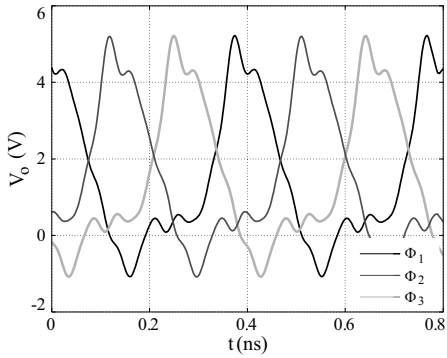

Figure 7. Voltage waveforms at the transistor drain port for different working points.

are located at the limits of the locking range (Φ_1 and Φ_3), and about its center (Φ_2). Since the efficiency of the synchronized solutions is practically independent of the values of P_r and f_r, the obtained voltage waveforms are almost identical to that represented in Fig. 4, corresponding to the optimized free running oscillator. Notice the phase difference between the traces, which is due to the fact that each one corresponds with a different value of $\Delta\phi$. The voltage and current waveforms associated with the working points located at the limits of locking range (Φ_1 and Φ_3) have been represented in Fig. 8, with $P_r = -40\,\text{dBm}$ (a), and $P_r = -20\,\text{dBm}$ (b). The phase difference between them has been eliminated to compare the amplitude difference between voltage and current waveforms at these working points. Note that both results are very similar, since the efficiency hardly changes throughout the synchronization loci.

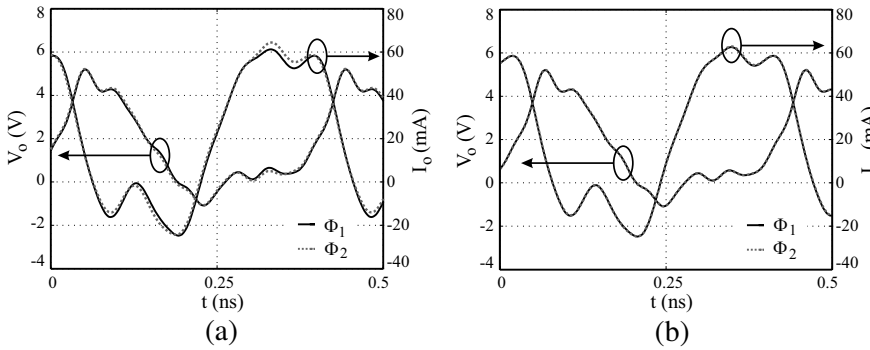

Figure 8. Comparison between the voltage and current waveforms evaluated at the limits of the locking range. (a) $P_r = -20\,\text{dBm}$. (b) $P_r = -40\,\text{dBm}$.

5.2. Phase-shifter Behavior of the ILVCO

The ILVCO can also works as continuous range electronically tunable phase shifter. In this case, the frequency of the reference signal is kept constant and the varactor diode included as part of the feedback network is used to slightly modify the free running frequency of the autonomous signal. Therefore, the phase difference $\Delta\phi = \phi_o - \phi_r$ between the autonomous and the reference signals can be adjusted.

Since ϕ_r can be arbitrarily set to zero, the synchronized solutions are found by sweeping the variable $\Delta\phi = \phi_o = \phi_{AG}$ between 0 and 360°, calculating for each point of the swept the values of the amplitude

of the autonomous signal $V_o = V_{AG}$ and the varactor capacity C_{var} for which the AG non perturbation condition is fulfilled.

Figure 9(a) represents the synchronized solutions, expressed in terms of ϕ_o and C_{var} for different values of the reference signal power P_r. The associated efficiency values have been represented in Fig. 9(b). As in the previous case, the obtained efficiency is very close to the optimum value reached for the free running oscillator, and the variation along the locking range and versus the reference signal power is very small.

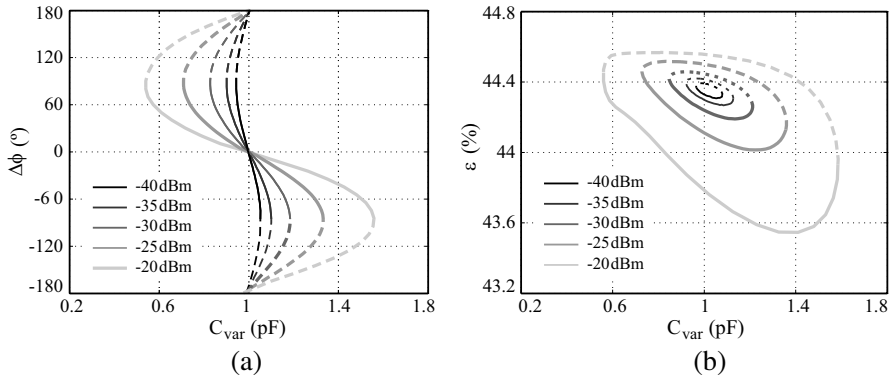

Figure 9. (a) Phase shifter synchronized solutions expressed in terms of the output phase and C_{var}, for different values of P_r. (b) Efficiency associated with the synchronized solutions. Continuous line: Stable solutions. Dashed line: unstable solutions.

The voltage and current waveforms of the output signal, obtained when the working point of the circuit is located at the limits of the locking range, with $P_r = -20\,\text{dBm}$ and $P_r = -40\,\text{dBm}$, have been represented in Fig. 10. The phase difference between them has been eliminated to show the minimum amplitude difference between voltage and current waveforms at these working points. This justify the minimum variation in the efficiency values throughout the synchronization loci. Note that both results are very similar to those achieved after the optimization of the free running oscillator, since the efficiency hardly changes.

6. EXPERIMENTAL RESULTS

A high efficiency ILVCO prototype with $f_o = 2.5\,\text{GHz}$ has been manufactured on Rogers 3003 substrate, with $\epsilon_r = 3$, in order to validate the proposed design approach. Before manufacturing the

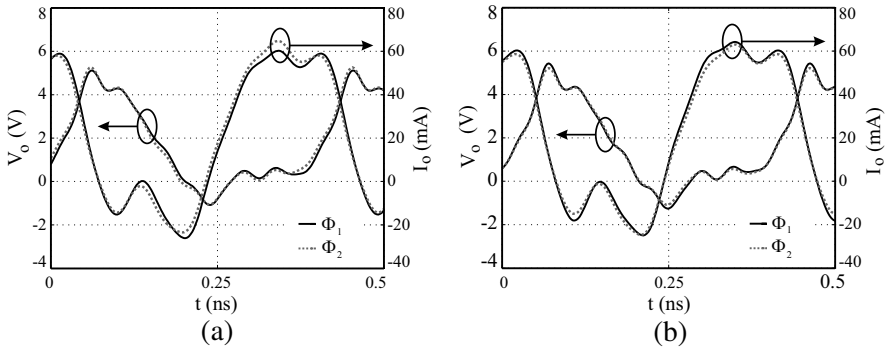

Figure 10. Comparison between the voltage and current waveforms evaluated at the limits of the phase shifter locking range. (a) $P_r = -20\,\text{dBm}$. (b) $P_r = -40\,\text{dBm}$.

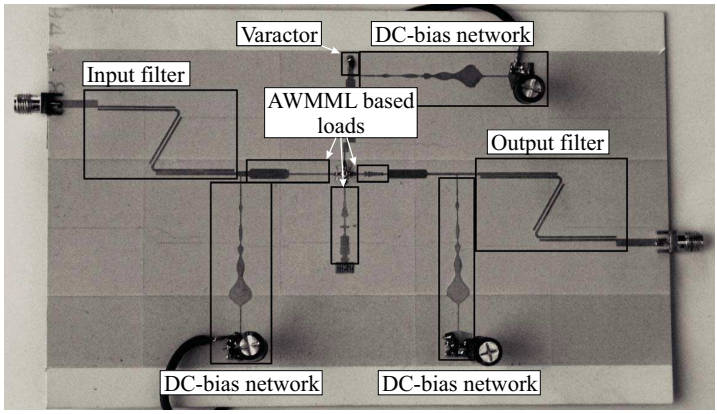

Figure 11. Picture of the manufactured prototype.

prototype, the frequency response of all the passive networks have been calculated in an electromagnetic simulation based on the Method of Moments, and slightly corrected when necessary. Fig. 11 shows a picture of the prototype.

6.1. Free Running Efficiency

When the circuit works under free running regime, the varactor diode voltage control is used to adjust the autonomous signal frequency f_o, providing a 19 MHz tuning range. The free running oscillator efficiency has been experimentally determined by loading the input

port with a matched termination, and measuring the power P_o of the autonomous signal fundamental component with a frequency spectrum analyzer. In order to obtain an accurate output power value, the losses of the measurement cables, transitions and circuit connectors have been carefully characterized. The measured power value at $f_o = 2.5\,\text{GHz}$ is $P_o = 11.4\,\text{dBm}$ when the DC drain voltage and current are $V_{drain} = 1.5\,\text{V}$ and $I_{drain} = 20\,\text{mA}$, respectively. Therefore, the obtained efficiency value is around $\epsilon = 46\%$.

6.2. Synchronized Solutions

The synchronized behavior of the high efficiency ILVCO has been characterized by using an Agilent PNA-X Vector Network Analyzer (VNA). The VNA is used to generate the input reference signal and to measure the ILVCO output signal. Since the frequency and the power of the generated reference signal can be controlled, the stable synchronized solutions are automatically obtained. Fig. 12 shows the measured solutions, in terms of the oscillator output power P_o (a) and phase $\Delta\phi_{out}$, referred to that of the reference signal (b), when the power of the reference signal varies from $P_r = -40\,\text{dBm}$ to $P_r = -20\,\text{dBm}$ in 5 dB steps. As can be observed, the comparison between experimental and simulated synchronized solutions, which have been superimposed, shows a very good degree of accordance between them. The efficiency of the synchronized solutions has been determined from the measured values of P_o and the DC power consumption and is represented in Fig. 13, together with simulation data.

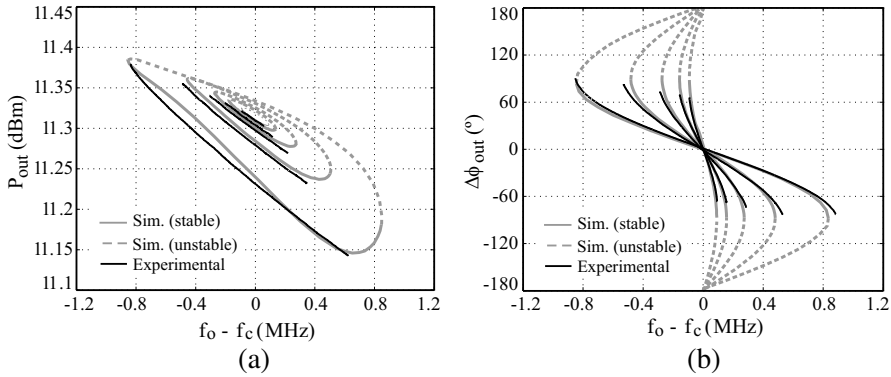

Figure 12. Measured synchronized solutions in terms of (a) the power P_o and (b) the phase $\Delta\phi_{out}$ of the output signal. The represented solutions have been obtained by changing the reference signal power P_r between -40 and $-20\,\text{dBm}$ in 5 dB steps.

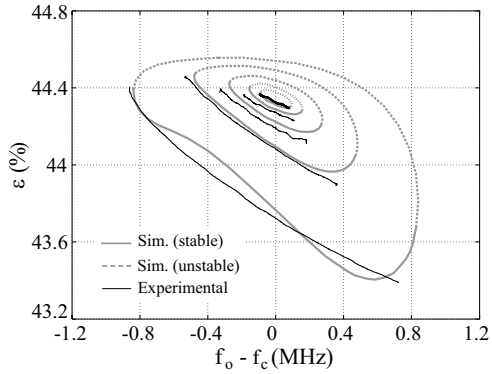

Figure 13. Measured efficiency of the synchronized solutions. The represented solutions have been obtained by changing the reference signal power P_r between -40 and -20 dBm in 5 dB steps.

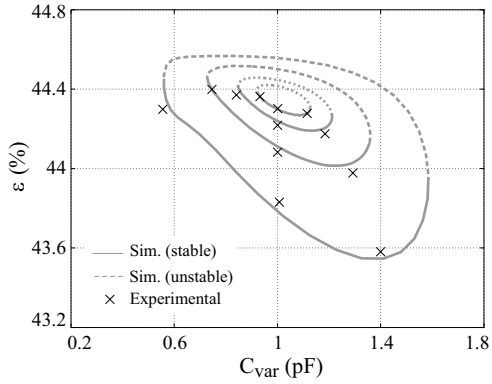

Figure 14. Measured efficiency of the phase shifter synchronized solutions. The represented solutions have been obtained by changing the reference signal power P_r between -35 and -20 dBm in 5 dB steps.

The synchronized solutions of the circuit working as variable phase shifter cannot be automatically obtained as described above, because the frequencies of the reference and the autonomous signals are equal and constant, and the phase difference between them, $\Delta\phi$, is controlled through the DC voltage applied to the varactor. In this case, the VNA is used to generate the reference signal and to measure the power and the phase of the oscillator output signal. The efficiency of such solutions has been represented in Fig. 14, together with simulation data.

7. CONCLUSIONS

A new approach for the optimization of the efficiency of an Injection Locked Voltage Controlled Oscillator (ILVCO), based on the use of an Auxiliary Generator, has been presented. The efficiency is taken as an additional optimization goal, which allows the direct control of its value. In addition, the high flexibility provided by multi-harmonic loads based on Arbitrarily Width Modulated Microstrip lines ensures the convergence of the optimization process. In this way, the efficiency of the autonomous solution is directly imposed on the circuit, while the existence of the desired autonomous solution is ensured, and the required design time is considerably reduced. To validate the described design technique, a 2.5 GHz ILVCO prototype has been manufactured and experimentally characterized, obtaining a good agreement between simulation and measurement data.

ACKNOWLEDGMENT

This work has been supported by the "Seventh Framework Programme of the European Commission" under project ICT-2011.8.2 600849 (INSIDDE), by the "Ministerio de Ciencia e Innovación" of Spain and "FEDER", under projects IPT-2011-0951-390000 (TECNIGRAF), TEC2011-24492 (ISCAT), TEC2008-01638 (INVEMTA), "CONSOLIDER-INGENIO CSD2008-00068" (TERASENSE) and grant AP2009-0438, by the "Plan de Ciencia y Tecnología" (PCTI/FEDER-FSE) of the "Gobierno del Principado de Asturias", under projects EQUIP08-06, FC09-COF09-12, EQUIP10-31 and PC10-06, and grant BP10-031, and by the "Cátedra Telefónica-Universidad de Oviedo".

REFERENCES

1. Deruyck, M., W. Verrecken, W. Joseph, B. Lannoo, M. Pickavet, and L. Martens, "Reducing the power consumption in wireless access networks: Overview and recommendations," *Progress In Electromagnetics Research*, Vol. 132, 255–274, 2012.
2. Shwe, H. Y., W. Peng, H. Gacanin, and F. Adachi, "Multi-layer WSN with power efficient buffer management policy," *Progress In Electromagnetics Research Letters*, Vol. 31, 131–145, 2012.
3. Dhar, J., S. K. Garg, R. K. Arora, and B. V. Bakori, "C-band pulsed solid state power amplifier for spaceborne applications," *Progress In Electromagnetics Research Letters*, Vol. 23, 75–87, 2011.

4. Thein, T. T., C. L. Law, and K. Fu, "Frequency domain dynamic thermal analysis in GaAs HBT for power amplifier applications," *Progress In Electromagnetics Research*, Vol. 118, 71–87, 2011.
5. Jiménez-Martín, J. L., V. González-Posadas, J. E. González-García, and F. J. Arqués-Orobón, "Dual band high efficiency class CE power amplifier based on CRLH diplexer," *Progress In Electromagnetics Research*, Vol. 97, 217–240, 2009.
6. El Maazouzi, L., A. Mediavilla, and P. Colantonio, "A contribution to linearity improvement of a highly efficient PA for WiMAX applications" *Progress In Electromagnetics Research*, Vol. 119, 59–84, 2011.
7. Chen, H., X. F. Ji, L. J. Jiang, and Y. X. Zhang, "Design and implementation of an X-band pulsed solid-state power amplifier with high power and high efficiency using radial waveguide combiner," *Progress In Electromagnetics Research C*, Vol. 21, 113–117, 2011.
8. Jahanbakht, M. and M. T. Aghmyoni, "LDMOS modelling and high efficiency power amplifier design using PSO algorithm," *Progress In Electromagnetics Research M*, Vol. 27, 219–229, 2012.
9. Bryerton, E. W., W. A. Shiroma, and Z. B. Popovic, "A 5 GHz high-efficiency class-E oscillator," *IEEE Microwave and Guided Wave Letters*, Vol. 6, No. 12, 441–443, 1996.
10. Moon-Que, L., S.-J. Yi, S. Nam, Y. Kwon, and K.-W. Yeom, "High-efficiency harmonic loaded oscillator with low bias using a nonlinear design approach," *IEEE Transactions on Microwave Theory and Techniques*, Vol. 47, No. 9, 1670–1679, 2009.
11. Kwok-Keung, M. C. and K.-P. Chan, "Power optimization of high-efficiency microwave MESFET oscillators," *IEEE Transactions on Microwave Theory and Techniques*, Vol. 48, No. 5, 787–790, 2000.
12. Ellinger, F., U. Lott, and W. Bächtold, "Design of a low-supply-voltage high-efficiency class-E voltage-controlled MMIC oscillator at C-band," *IEEE Transactions on Microwave Theory and Techniques*, Vol. 49, No. 1, 203–206, 2001.
13. Ver Hoeye, S., F. Ramrez, and A. Surez, "Nonlinear optimization tools for the design of high-efficiency microwave oscillators," *IEEE Microwave and Wireless Components Letters*, Vol. 14, No. 5, 189–191, 2004.
14. Sanggeun, J., A. Suárez, and D. B. Rutledge, "Nonlinear design technique for high-power switching-mode oscillators," *IEEE Transactions on Microwave Theory and Techniques*, Vol. 54, No. 10, 3630–3640, 2006.

15. Hwang, W. J., S. W. Shin, G. W. Choi, H. J. Kim, and J. J. Choi, "High-efficiency power oscillator using harmonic-tuned matching network," *IEEE MTT-S International Microwave Symposium Digest, MTT'09*, 1505–1508, 2009.
16. Shin, S. W., G. W. Choi, H. J. Kim, S. H. Lee, S. H. Kim, and J. J. Choi, "Frequency-tunable high-efficiency power oscillator using GaN HEMT," *2010 IEEE MTT-S International Microwave Symposium Digest (MTT)*, 1000–1003, 2010.
17. Massari, A. and E. Limiti, "5 GHz high efficiency oscillator with filtering feedback network," *Integrated Nonlinear Microwave and Millimetre-wave Circuits (INMMIC), 2011*, 1–4, 2011.
18. Lin, C. H., W. P. Li, and H. Y. Chang, "A fully integrated 2.4-GHz 0.5-W high efficiency class-E voltage controlled oscillator in 0.15-m PHEMT process," *Microwave Conference Proceedings (APMC), 2011 Asia-Pacific*, 864–867, 2011.
19. Berini, P., M. Desgagne, F. M. Ghannouchi, and R. G. Bosisio, "An experimental study of the effects of harmonic loading on microwave MESFET oscillators and amplifiers," *IEEE Transactions on Microwave Theory and Techniques*, Vol. 42, No. 6, 943–950, 1994.
20. Ver Hoeye, S., C. Vázquez, M. González, M. Fernández, L. F. Herrán, and F. Las Heras, "Multi harmonic DC-bias network based on arbitrarily width modulated microstrip line," *Progress In Electromagnetics Research Letters*, Vol. 11, 119–128, 2009.
21. Fernádez, M., S. Ver Hoeye, C. Vázquez, G. Hotopan, R. Camblor, and F. Las Heras, "Optimization of the synchronization bandwidth of rationally synchronized oscillators based on bifurcation control," *Progress In Electromagnetics Research*, Vol. 119, 299–313, 2011.
22. Ver Hoeye, S., L. F. Herrán, M. Fernández, and F. Las Heras, "Design and analysis of a microwave large-range variable phase-shifter based on an injection-locked harmonic self-oscillating mixer," *IEEE Microwave and Wireless Components Letters*, Vol. 16, No. 6, 342–344, 2006.
23. Vázquez, C., S. Ver Hoeye, M. Fernández, L. F. Herrán, and F. Las Heras, "Analysis of the performance of injection locked oscillators in a data transmitting polarisation agile antenna application," *Progress In Electromagnetics Research Letters*, Vol. 12, 1–10, 2009.
24. Fernádez, M., S. Ver Hoeye, C. Vázquez, G. Hotopan, R. Camblor, and F. Las Heras, "Design and analysis of a multi-carrier TX-RX system based on rationally synchronized oscillators for localization

applications," *Progress In Electromagnetics Research*, Vol. 120, 1–16, 2011.

25. Fernádez, M., S. Ver Hoeye, C. Vázquez, G. Hotopan, R. Camblor, and F. Las Heras, "New non-linear approach for the evaluation of the linearity of high gain harmonic self-oscillating mixers," *Progress In Electromagnetics Research*, Vol. 126, 149–168, 2012.
26. Fernádez, M., S. Ver Hoeye, C. Vázquez, G. Hotopan, R. Camblor, and F. Las Heras, "Non-linear optimization technique for the reduction of the frequency scanning effect in a phased array based on broadband injection-locked third harmonic self-oscillating mixers," *Progress In Electromagnetics Research*, Vol. 127, No. 10, 479–499, 2012.
27. González-Posadas, V., J. L. Jiménez-Martín, A. Parra-Cerrada, D. Segovia-Vargas, and L. E. García-Muñoz, "Oscillator accurate linear analysis and design. Classic methods review and comments," *Progress In Electromagnetics Research*, Vol. 118, 89–116, 2011.
28. Jimenez-Martin, J. L., V. Gonzalez-Posadas, A. Parra-Cerrada, D. Segovia-Vargas, and L. Garcia-Munoz, "Provisos for classic linear oscillator design methods. New linear oscillator design based on the NDF/RRT," *Progress In Electromagnetics Research*, Vol. 126, 17–48, 2012.
29. Jimenez-Martin, J. L, V. Gonzalez-Posadas, A. Parra-Cerrada, A. Blanco-del-Campo, and D. Segovia-Vargas, "Transpose return relation method for designing low noise oscillators," *Progress In Electromagnetics Research*, Vol. 127, 297–318, 2012.